

A search for yellow young disk population stars among EMSS stellar X-ray sources by means of lithium abundance determination*

F. Favata¹, M. Barbera², G. Micela², and S. Sciortino²

¹ Astrophysics Division - ESA/ESTEC, Postbus 299, NL-2200 AG Noordwijk, The Netherlands

² Osservatorio Astronomico di Palermo, Piazza del Parlamento 1, I-90134 Palermo, Italy

Received February 11, accepted May 31, 1993

Abstract. Using previous radial velocity surveys of the EMSS stellar sample which have identified most of the detectable active binary systems, including X-ray luminous RS CVn type systems, we have selected a sample of apparently normal, mostly single EMSS stars with spectral type comprised between F5 and K8. We have studied this sample by means of high resolution spectral observations with the aim of measuring their photospheric Li abundances and, therefore, their age distribution. Our results support the hypothesis, based on a model of the stellar coronal component of the Galaxy, that, to be consistent with the accepted values for the stellar birthrate in the last billion years, a considerable fraction of the “normal” yellow stars detected in the EMSS must be young objects with ages comparable to the Pleiades.

Key words: stars: abundances – stars: late-type – X-rays: stars – galaxy: stellar content

1. Introduction

The analysis of the content of the stellar component of serendipitous flux-limited X-ray surveys is a powerful tool for the study of the stellar population in the Galaxy, and can be used, among other things, to study the global characteristics of stellar X-ray emission and to put powerful constraints on the stellar birth rate in the Galaxy.

Using a model of the Galaxy based on the Bahcall and Soneira “standard” Galaxy model (Favata et al. 1992) and on X-ray luminosity functions for age-homogeneous groups of stars obtained from *Einstein* observations, Micela et al. (1993) have shown that, given the strong age dependence of X-ray luminosity, the content of late-type stellar coronal sources in X-ray flux

limited surveys can be used to put constraints on the stellar birth rate in the Galaxy in the last billion years. In particular, to be compatible with most other independent birth rate determinations, the Extended Medium Sensitivity Survey (EMSS) must contain a substantial fraction of “normal” coronal sources with ages similar to the Pleiades or younger. An investigation of the age of a representative sample of EMSS sources can therefore supply an independent check of the consistency of the approach of Micela et al. (1993). This is also a way of identifying a sample of active stars well characterized in age, to be the subject of future, more detailed investigations on the dependency of X-ray emission on stellar age.

A sub-sample of the EMSS coronal component has been studied down to a certain level of detail by Fleming (1988) and Fleming et al. (1989a, 1989b), who searched the sample for evidence of radial velocity variations (as an indicator of multiplicity) and for evidence of spectral peculiarities. They identified a number of candidate “peculiar” sources, such as RS CVn binaries, FK Com stars and W UMa binaries, thus leaving a “clean” sub-sample of apparently normal coronal sources, which constitute a good starting point for our investigation. We have therefore conducted a campaign of high resolution spectroscopic observations of the Li I 6708 Å line in a substantial sample of EMSS yellow stars in order to determine their Li abundance and thereby their age.

The main observational result of this paper is that objects with a high Li abundance are quite common among EMSS yellow stars. The role of Li as an age indicator has recently been questioned, in the light of the discovery of relatively high Li abundances in objects which, on the basis for example of evolutionary arguments, should be old and therefore have a very low Li abundance. Examples are the high Li giants of Gratton & D’Antona (1989). There are also indications that Li abundances higher than expected on the basis of the evolutionary status are present in “active” stellar systems. This seems to be specially true in active binaries, such as RS CVn binary systems (Pallavicini et al. 1992). As we have tried to select a sample composed mainly of single stars, such effects should have

Send offprint requests to: F. Favata

* Based on observations collected at the ESO La Silla and DAO Victoria observatories

little influence on our sample. Given the above caveat the Li abundances presented in this paper should not be taken at face value as indicative of stellar age in every case. Nevertheless, we show that for a significant fraction of the observed stars, the Li abundances are high enough to be compatible with stellar ages similar (or younger than) the Pleiades open cluster. In several cases, the Li abundance is consistent with the star still being in the pre-main sequence stage.

This paper is structured as follows: in Sect. 2 the observed sample is described. The observations are presented and the data reduction and analysis procedure are discussed in Sec. 3. The results are then presented, followed by a discussion. Our conclusions and plans for future work are summarized in Sec. 7. Notes on individual stars are collected in the Appendix.

2. The observed sample

To conduct our investigation one would ideally have wanted to observe the entire sample of Extended Medium Sensitivity Survey sources with spectral types F, G and K. We have in practice restricted our sample to the brighter stars ($m_v \leq 12.0$) of the Extended Medium Sensitivity Survey, although we hope to extend our survey to fainter magnitudes in the future. Of the 222 stars which form the complete EMSS stellar sample, 158 are classified as F, G or K type. Of these, 135 are brighter than $m_v = 12.0$. Of these 135, 67 have been observed in the course of our program.

Table 2 lists the observed sample, together with the available optical information, mostly taken from the literature (color, spectral type, magnitude) for each object. Aside from brightness and observability constraints the sample was chosen largely at random, and should therefore be representative of the entire Extended Medium Sensitivity Survey sample in the appropriate magnitude range.

3. Observations and data reduction

The observations presented here were obtained at the European Southern Observatory (ESO) La Silla during July 1991 and September 1992 and at the Dominion Astrophysical Observatory (DAO) during June 1992. At ESO the observations were performed using the 1.44 m CAT telescope and the Coude Echelle Spectrograph (CES) with the short camera and the RCA (ESO #9) CCD, at about 2.6 Å/mm dispersion, corresponding to a resolving power of approx. 50 000 as measured on Th-Ar lamp exposures. At DAO the 1.22m telescope and Coude Spectrograph were used, with the 830 grooves/mm grating at first order, the 96 in. camera, the IS32R image slicer and the PM512 CCD. Dispersion was 4.8 Å/mm, yielding an effective resolving power of about 30 000.

All the spectra were taken in a region centered on the Li I 6708 Å line, and covered about 45 Å for both the CAT and DAO observations. Standard data reduction (bias subtraction, flat fielding, spectrum extraction and wavelength calibration) was performed using the IRAF software package. Given that many CCD chips are known to have fringing problems in the

red spectral regions (and the ESO #9 CCD is well known to exhibit fringing), three different flat fielding techniques were used. Flat field exposures were obtained by using the internal spectrograph calibration lamps, by taking external flat field exposures using dome lamps and by observing bright B stars with high rotational velocity, which have basically flat spectra in the region observed. Representative data covering the whole range of observed signal to noise ratios from each observing run have been reduced using the three different flat field exposures. No appreciable difference in the flat fielding obtained with the three procedures was observed at the signal to noise ratio of our observation, and therefore all of the observation were processed using internal flat field exposures.

The Li I 6707.81 Å line is very close to the Fe I 6707.44 Å line and it is often blended with it, because of spectral line broadening caused by stellar rotation. To evaluate the contribution of the Fe I line to the blend for the cases in which the lines could not be resolved we have used the sample of Pallavicini et al. (1992), who observed a number of bright stars with essentially the same spectrograph configuration as our program stars, and evaluated the equivalent width of the Fe I 6707.44 Å line. To check the consistency of our data with the data of Pallavicini et al. (1992) we have re-observed some of their calibration stars, noting essentially no difference between the Fe I 6707.44 Å equivalent width reported by them and our measurements. The equivalent width of the Fe I line is plotted in Fig. 1 for our calibration stars (which include the sample of Pallavicini et al. (1992) plus our re-observations), against effective temperature. It is evident that a monotonical relationship (although perhaps not a perfectly linear one) exists between the equivalent width of the Fe I 6707.44 Å and effective temperature. The scatter can be explained as due to either errors in the assumed effective temperature as well as to differences in metallicity among the comparison stars.

After the reduction process described above the equivalent width of the Li I 6707.81 Å was measured, using the tasks provided within the IRAF *splot* software package. For stars with narrow enough lines to have the Li I 6707.81 Å line sufficiently separated from the nearby Fe I 6707.44 Å line, the equivalent width of each of the partially blended lines was determined using the two-Gaussian fitting routine of the package. In the cases in which stellar rotation blends the lines to the point to which they are no longer distinguishable, we have measured the equivalent width of the Fe I + Li I blend, from which the equivalent width of the Fe I line at the appropriate effective temperature from the fit of Fig. 1 was afterwards subtracted.

For those cases in which no Li line was visible in the spectrum we used the statistical noise measured on the continuum of the spectrum to determine an upper limit to the Li line equivalent width. The situation is more complex in the case of Li+Fe blends, as it is not possible to distinguish Li line detections from upper limits. In four cases the equivalent width of the blend is within 50% of the “predicted” equivalent width of the Fe line, resulting in very small (or negative) residual Li equivalent widths. Given the relatively large error of the predicted values of the Fe abundance, we have considered these cases as non-detections,

Table 1. Optical information about the observed sample. See notes at the end of the table for information about individual columns

MS name	Other name	V mag.	spectral type	$T_{\text{eff}}(K)$	+/-	notes
MS 0002.8+1602	SAO 91699	8.6	F5V	6500	100	
MS 0003.3-4201	SAO 214961	7.4	G0V	5920	150	*
MS 0009.9+1407	SAO 91772	8.5	G5V	5300	200	*
MS 0011.6+0840	–	11.5	K0Ve	4650	100	
MS 0031.9-0646	SAO 128830	6.8	F4V	6600	200	
MS 0132.5+2101	–	10.8	F9V	5920	100	*
MS 0134.4+2027a	SAO 74827	8.7	F9V	5580	100	*
MS 0134.4+2027b	SAO 74827	8.7	F9V	5580	100	*
MS 0138.0-5627	HD 10360	5.8	K5V	4410	250	
MS 0206.2-1019	–	8.9	G5V	5610	100	
MS 0234.2-0321	SAO 130011	8.1	K2V	4750	100	
MS 0234.8-0210	–	10.4	G9V	5400	100	
MS 0236.4-0148a	SAO 130032	9.0	F8V	6200	300	*
MS 0236.4-0148b	SAO 130032	9.0	F8V	6200	300	*
MS 0236.4-0148c	SAO 130032	9.0	F8V	6200	300	*
MS 0239.9+0704	SAO 110699	8.9	K5V	4410	300	
MS 0244.9-0024	SAO 130113	9.6	G9V	5300	100	
MS 0257.4+0733	SAO 110894	7.9	G6III	5010	100	
MS 0300.1-1528a	SAO 148731	8.4	G8V	5000	100	*
MS 0300.1-1528b	SAO 148731	8.4	G8V	5000	100	*
MS 0303.8+1717	SAO 93280	8.7	F7V	6300	200	
MS 0307.5+1424	–	10.4	G6V	5500	100	*
MS 0308.3+1413	–	11.4	F8V	5780	100	
MS 0315.7-1955	–	10.8	K5V	5300	100	*
MS 0318.5-1926	–	10.3	K7V	4600	100	
MS 0326.6-2008	SAO 168572	10.1	F4V	6600	200	
MS 0327.2-2416	SAO 168581	9.1	K7V	4160	300	
MS 0333.1+0607	–	10.3	F6V	6300	100	
MS 0337.6-0202	SAO 130647	8.0	G9V	5400	300	
MS 0348.2-1404a	–	10.7	K0IV	5300	100	*
MS 0348.2-1404b	–	10.7	K0IV	5300	100	*
MS 0413.7-6235	SAO 248969	3.4	G8III	4870	200	
MS 0438.5+0213	–	10.6	F9V	5000	100	*
MS 0443.8-1006	–	11.8	K7V	4400	100	
MS 0443.8-1006	–	11.8	K7V	4400	100	
MS 0448.4+1058	SAO 94163	6.8	F8V	6200	300	*
MS 0452.2+0225	–	10.6	K0V	5240	300	
MS 0457.5+0312	SAO 112298	7.5	K2V	4780	200	
MS 0505.0-0527	–	10.2	G9IV	4850	100	
MS 0515.4-0710	–	10.8	K2e	4780	200	*
MS 0519.3-4544	–	11.8	K8Ve	4000	300	*
MS 0535.7-2839	SAO 170610	7.2	F4V	6600	200	*
MS 0538.5-0949	SAO 132453	8.6	F8V	5700	100	
MS 0617.0-5847	SAO 234435	8.7	F5	6540	100	*
MS 0648.1-5042	–	11.9	K3V	4700	300	*
MS 1100.2+6155	SAO 15379	7.1	F8	6200	100	
MS 1109.8+3606	SAO 62451	6.4	G0V	5920	100	
MS 1254.8+0142	SAO 119684	7.0	F4V	6600	200	
MS 1256.2+3833	–	9.3	K3V	4700	200	
MS 1309.7+3221	SAO 63396	6.7	F8	6200	200	

Table 1. (continued)

MS name	Other name	V mag.	spectral type	$T_{\text{eff}}(K)$	+/-	notes
MS 1330.5-0811	SAO 139405	7.2	G0V	5920	100	
MS 1436.8-2628	SAO 182743	9.7	K4V	4500	300	
MS 1441.7+5208	SAO 29254	8.2	G2V	5700	100	
MS 1520.7-0625	SAO 140499	7.3	K0III	4720	200	*
MS 1521.1+3027	SAO 64673	5.6	F8V	6000	100	
MS 1552.0-2338	SAO 183920	8.8	G3IV	5700	200	*
MS 1558.4-2232	–	11.4	K3e	4700	300	*
MS 1634.7+2638	SAO 84485	8.0	F5V	6540	200	
MS 1704.3+5432	SAO 30239	5.8	F6V	6500	100	
MS 1737.2+6847a	SAO 17576	4.8	F5V	6540	100	*
MS 1737.2+6847b	SAO 17576	4.8	F5V	6540	100	*
MS 1751.0+7045	–	9.6	K5IV	4410	200	*
MS 1753.5+1830	SAO 103221	9.2	K4	4500	300	
MS 1810.3+6940	SAO 17800	8.6	K2V	4780	200	
MS 1906.8-6339	–	11.2	K5	4410	300	
MS 1907.0-6405	–	11.8	K4V	4500	300	
MS 2148.2+1420	–	11.4	K3IV/V	4600	300	
MS 2254.2+0219	–	10.3	K2V	4400	200	
MS 2302.4-4427	SAO 231427	9.7	G8	5490	300	
MS 2315.1-3640	–	11.3	K2V/K4V	4600	300	
MS 2332.4+0119	GJ 900	9.5	M1V	3680	100	
MS 2335.2+0305	SAO 128293	7.3	F5V	6540	250	
MS 2349.8-0112	–	10.7	K0III	5500	100	*
MS 2349.8-0112	–	10.7	K0III	4720	300	*

Notes to Table 1: the first column is the name from EMSS catalog. In the case of SB2 systems a lower case letter has been appended to the name to distinguish the various components. The second column lists, when available, the object name from other catalogs. Column three and four list the visual magnitude and spectral type from Stocke et al. (1991), columns five and six list the assumed effective temperature from the color information (where available) or from the spectral type and the assumed error on the temperature, computed as described in the text. An asterisk in column six indicates that the star is discussed in more detail in the Appendix.

and we do not report a Li abundance in Table 2. They are furthermore not plotted in Fig. 3.

The equivalent widths were converted to Li abundances by using the published curves of growth of Pallavicini et al. (1987). We have interpolated the published curves of growth using a 2-d cubic spline interpolator. A few of our sample objects have an effective temperature that falls just outside the 4500-6500 K range of the Pallavicini et al. (1987) curves of growth. In these cases we used the same 2-d cubic spline to extrapolate the curve of growth. These extrapolated cases should be treated with caution.

The largest uncertainty in the Li abundances computed in this way stems from the uncertainty in the estimated effective temperature. The effective temperatures of the program stars were estimated from published B-V colors, when available, or from published spectral type if no color information was available, using a spline fit to the table of Zombeck (1990). Unless otherwise quoted in the original source, we have assumed an error of 0.1 in published B-V colors and an error of two subtypes in published spectral types. This assumed uncertainty has been propagated into the effective temperature and the Li abundance, and is the uncertainty listed in Table 2. Admittedly, this uncer-

tainty is relatively large, and could be decreased by a more accurate effective temperature determination by photometric means. Nevertheless, as the conclusions of this work are based on the statistical properties of the observed sample, rather than on the precise determination of the Li abundance of any given source, we felt that such an improvement in the determination of effective temperatures is not fundamental for the purposes of this paper.

In the case of spectroscopic binaries (SB2) in which the two Li spectral lines are clearly separated, the correct approach is to separately measure the apparent equivalent width of each of the two lines, scaling it afterwards to the appropriate continuum contribution of each of the two sources. To do this it is necessary to estimate both the effective temperature and the radius of each of the components. Unfortunately for none of the cases in our sample (which include one triple system) are separate estimates for the spectral type or color of each of the components available in literature. Given that in all cases the spectra of each of the components and the relative intensity of the lines are similar we have assumed that all the components in the observed multiple systems have the same spectral type and effective temperature, i.e. they contribute equally to the continuum. While

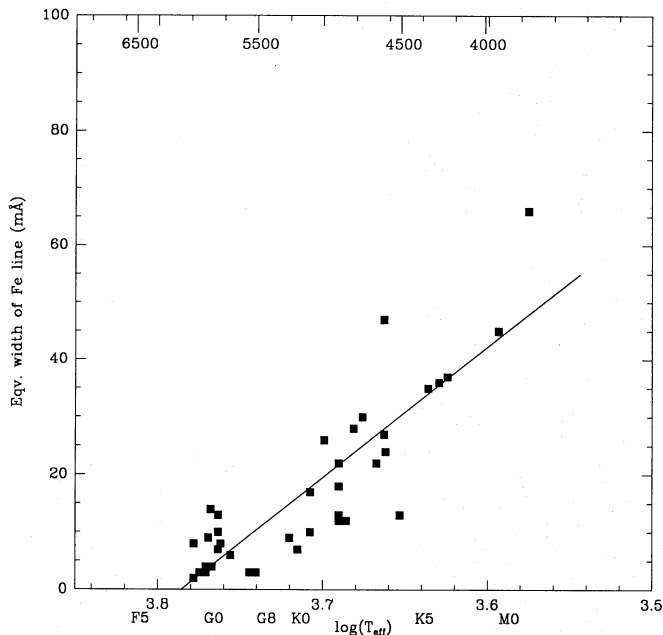


Fig. 1. Fe I 6707.44 Å equivalent width for normal main sequence stars versus effective temperature, for a sample of comparison stars observed by Pallavicini et al. (1992), some of which have been re-observed by us. The continuous line is the fit we have used to estimate the contribution of Fe I to the Li I + Fe I blend for program stars

this is the best one can do with the available information, this procedure is likely to introduce additional errors. Therefore in Fig. 3 such systems are flagged with a different (filled) symbol. For two cases (MS 0348.2-1404 and MS 1737.2+6847) the derived Li abundances for the components of multiple systems are not compatible, pointing to the components not being similar. All multiple systems are individually discussed in the Appendix.

4. Comparison sample

To compare the Li abundance of our sample stars with the Li abundances of stars of known age in an homogeneous way, we have reprocessed the Li data available from the literature for samples of stars from the Hyades and Pleiades open clusters (from Duncan & Jones 1983) and from the Taurus-Auriga star formation region (from Basri et al. 1991), using the same procedure as for our own data. For the Hyades and Pleiades data Duncan & Jones (1983) report both the $B - V$ color and the observed equivalent width of the Li line. In this case we have converted the $B - V$ color to effective temperature using the relation given by Zombeck (1990), and then computed the Li abundance using the curves of growth of Pallavicini et al. (1987), exactly in the same way as for our sample. This produces Li abundance values homogeneous to our own values. In the case of the Taurus-Auriga sample of 1991 only the effective temperature is given in the literature, with no color information. Therefore we have computed the Li abundances from the same curves of growth of Pallavicini et al. (1987) using the effective

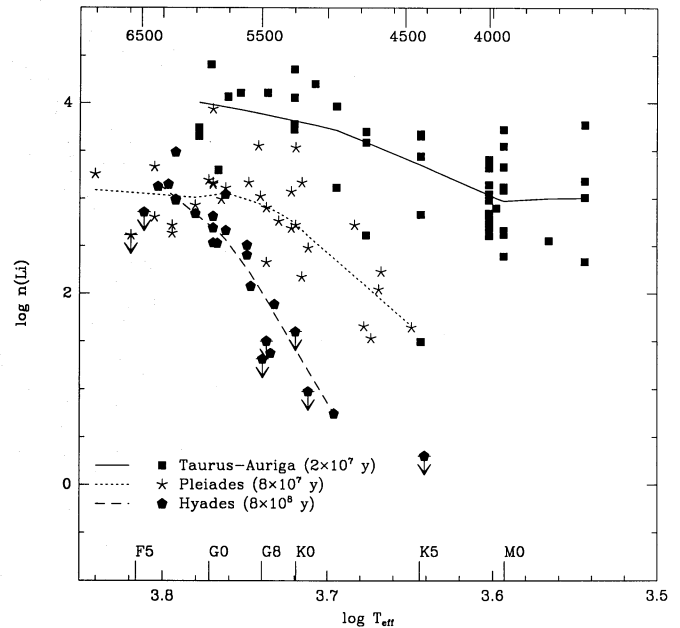


Fig. 2. Li abundances re-computed for the Hyades and Pleiades samples of Duncan & Jones (1983) and for the sample of pre-main sequence stars from the the Taurus-Auriga cloud of Basri et al. (1991). The separate robust fits for each sample, obtained as described in the text are also shown. Upper limits to the Li abundance are identified by down-pointing arrows

temperatures and equivalent widths published by Basri et al. (1991).

The above procedure resulted in a comparison sample which is as homogeneous as possible to our own data, although perhaps not necessarily processed in the best of all possible ways (i.e. an atmospheric analysis would perhaps produce more accurate values for the Li abundance). For each of the three comparison samples we computed robust fits to the data points, using the algorithm of Cleveland (1979). The algorithm, which ignores outliers, has been modified to take into account upper limits. The data points for three comparison samples are plotted in Fig. 2, together with the robust fits. The fits are only defined between values of T_{eff} bounded by the highest and lowest detected values (as opposed to upper limits) of Li abundance. Note that the fits for the Pleiades and Hyades samples cross close to 6400 K. Given that that is the region in T_{eff} for which the “hiatus” in Li values for the Hyades reported by Boesgard (1987) appears, and that there are no detections in the sample of Duncan & Jones (1983) blueward of 6400 K, this should not be taken as significant.

5. Results

Fig. 3 shows the Li abundances computed for our observed sample plotted as $\log n(\text{Li})$ against $\log T_{\text{eff}}$, on the usual scale where $\log n(\text{H}) = 12.00$. Also shown in the plot are the robust fits for the Hyades and Pleiades open clusters and for the pre main sequence stars from the Taurus-Auriga star forming region

Table 2. Results of the Li abundance analysis. See notes at the end of the table for details about individual columns

MS name	T_{eff} (K)	+/-	W(Li)	W(Fe)	W(blend)	up/det	W(Fe) blend	log n(Li)	+/-
MS 0002.8+1602	6500	100	.025	.025	–	det	–	2.50	0.10
MS 0003.3-4201	5920	150	.152	.003	–	det	–	3.40	0.15
MS 0009.9+1407	5300	200	–	–	.042	–	0.0167	1.35	0.20
MS 0011.6+0840	4650	100	–	–	.160	–	0.0298	1.75	0.10
MS 0031.9-0646	6600	200	–	–	.046	–	0.0000	2.95	0.20
MS 0132.5+2101	5920	100	–	–	.195	–	0.0028	3.75	0.10
MS 0134.4+2027a	5580	100	–	–	.050	–	0.0070	1.95	0.15
MS 0134.4+2027b	5580	100	–	–	.038	–	0.0070	1.75	0.15
MS 0138.0-5627	4410	250	.002	.007	–	up	–	-0.95	0.20
MS 0206.2-1019	5610	100	.005	.005	–	up	–	0.95	0.10
MS 0234.2-0321	4750	100	.005	.014	–	up	–	-0.05	0.10
MS 0234.8-0210	5400	100	.009	.068	–	det	–	1.00	0.10
MS 0236.4-0148a	6200	300	–	–	.027	–	0.0000	2.25	0.30
MS 0236.4-0148b	6200	300	–	–	.023	–	0.0000	2.15	0.30
MS 0236.4-0148c	6200	300	–	–	.021	–	0.0000	2.10	0.30
MS 0239.9+0704	4410	400	.059	.025	–	det	–	0.75	0.30
MS 0244.9-0024	5300	100	.015	.065	–	det	–	1.10	0.10
MS 0257.4+0733	5010	100	–	.019	–	up	–	-0.35	0.10
MS 0300.1-1528a	5000	100	.008	.014	–	up	–	0.50	0.10
MS 0300.1-1528b	5000	100	.008	.010	–	up	–	0.50	0.10
MS 0303.8+1717	6300	200	–	–	.010	–	0.0000	1.90	0.20
MS 0307.5+1424	5500	100	.200	.008	–	det	–	3.50	0.15
MS 0308.3+1413	5780	100	–	–	.020	–	0.0039	1.15	0.10
MS 0315.7-1955	5300	100	–	–	.395	–	0.0157	4.30	0.15
MS 0318.5-1926	4600	100	–	–	.093	–	0.0302	1.05	0.10
MS 0326.6-2008	6600	200	–	–	.040	–	0.0000	2.90	0.20
MS 0327.2-2416	4160	300	–	–	.010	–	0.0398	–	–
MS 0333.1+0607	6300	100	–	–	.084	–	0.0000	3.10	0.10
MS 0337.6-0202	5400	300	.015	.040	–	up	–	1.20	0.20
MS 0348.2-1404a	5300	100	–	–	.064	–	0.0157	1.95	0.25
MS 0348.2-1404b	5300	100	–	–	.120	–	0.0157	2.45	0.25
MS 0413.7-6235	4870	200	.050	.018	–	det	–	1.30	0.20
MS 0438.5+0213	5000	100	–	–	.030	–	.0186	0.65	0.10
MS 0443.8-1006	4400	100	.045	.015	–	det	–	0.55	0.10
MS 0443.8-1006	4400	100	.045	.015	–	det	–	0.55	0.10
MS 0448.4+1058	6200	300	.064	.008	–	det	–	2.75	0.25
MS 0452.2+0225	5240	300	.031	.015	–	det	–	1.40	0.20
MS 0457.5+0312	4780	200	–	–	.171	–	0.0225	2.05	0.25
MS 0505.0-0527	4850	100	–	–	.120	–	0.0215	1.70	0.10
MS 0515.4-0710	4780	200	–	–	.250	–	0.0225	2.70	0.15
MS 0519.3-4544	4000	300	–	–	.110	–	0.0398	0.25	0.20
MS 0535.7-2839	6600	200	–	–	.125	–	0.0000	3.75	0.20
MS 0538.5-0949	5700	100	–	–	.135	–	0.0047	3.00	0.10
MS 0617.0-5847	6540	100	–	–	.050	–	0.0000	2.95	0.15
MS 0648.1-5042	4700	300	–	–	.380	–	0.0302	3.25	0.25
MS 1100.2+6155	6200	100	–	–	.095	–	0.0000	3.05	0.15
MS 1109.8+3606	5920	100	.010	.028	–	up	–	1.50	0.10
MS 1254.8+0142	6600	200	–	–	.015	–	0.0000	2.40	0.20
MS 1256.2+3833	4700	200	–	–	.090	–	0.0302	1.15	0.20
MS 1309.7+3221	6200	200	–	–	.013	–	0.0000	1.90	0.20

Table 2. (continued)

MS name	T_{eff} (K)	+/-	W(Li)	W(Fe)	W(blend)	up/det	W(Fe) blend	log n(Li)	+/-
MS 1330.5-0811	5920	100	.070	.005	–	det	–	2.55	0.10
MS 1436.8-2628	4500	400	.010	.007	–	up	–	-0.05	0.20
MS 1441.7+5208	5700	100	–	–	.120	–	0.0031	2.85	0.10
MS 1520.7-0625	4720	200	–	–	.037	–	0.0340	–	–
MS 1521.1+3027	6000	100	–	–	.059	–	0.0012	2.55	0.10
MS 1552.0-2338	5700	200	–	–	.250	–	0.0051	4.05	0.30
MS 1558.4-2232	4700	300	–	–	.341	–	0.0263	3.10	0.30
MS 1634.7+2638	6540	200	–	–	.020	–	0.0000	2.45	0.20
MS 1704.3+5432	6500	100	–	–	.020	–	0.0000	2.45	0.10
MS 1737.2+6847a	6540	100	–	–	.032	–	0.0000	2.70	0.25
MS 1737.2+6847b	6540	100	–	–	.058	–	0.0000	3.05	0.25
MS 1751.0+7045	4410	200	–	–	.080	–	0.0223	0.75	0.20
MS 1753.5+1830	4500	300	.007	.008	–	up	–	-0.20	0.20
MS 1810.3+6940	4780	200	.014	.013	–	det	–	0.45	0.20
MS 1906.8-6339	4410	300	.070	.001	–	det	–	0.85	0.20
MS 1907.0-6405	4500	300	–	–	.045	–	0.0321	0.05	0.20
MS 2148.2+1420	4600	300	–	–	.150	–	0.0263	1.60	0.30
MS 2254.2+0219	4400	200	–	–	.127	–	0.0225	1.15	0.30
MS 2302.4-4427	5490	300	–	–	.025	–	0.0111	1.25	0.30
MS 2315.1-3640	4600	300	–	–	.020	–	0.0283	–	–
MS 2332.4+0119	3680	100	–	–	.032	–	0.0408	–	–
MS 2335.2+0305	6540	250	.004	.004	–	up	–	1.75	0.20
MS 2349.8-0112	5500	100	–	–	.235	–	0.0089	3.75	0.30
MS 2349.8-0112	4720	300	–	–	.235	–	0.0302	2.45	0.30

Notes to Table 2: all the equivalent widths are in Å. Columns 2 and 3 list the effective temperature used to compute the Li abundance. Columns 4 and 5 list the measured equivalent widths of the Li 6707.81 and Fe 6707.44 lines in those cases in which they are clearly separated. Column 6 gives the measured equivalent width of the blend of the two lines for the cases where the lines are blended. Column 7 has a value of either *up* or *det*, depending on whether the Li line was detected or not. This is relevant only for the cases in which the lines were not blended. Column 8 is the predicted equivalent width of the Fe line, from the fit of Fig. 1, which has been subtracted from the blended equivalent width. Columns 9 and 10 list the computed Li abundance with the assumed uncertainty, computed as described in the text, in the usual scale in which $\log n(\text{H}) = 12.00$.

computed as described in Sect. 4. The results of our curve of growth analysis are listed in detail in Table 2.

The Li 6707.44 Å line is formed very far out in the stellar atmosphere, where stellar atmosphere models have not been tested extensively (none of the current models takes into account the presence of the chromosphere of active stars), and where scattering and possibly departures from LTE may influence line formation. Additionally, for pre-main sequence stars, the equivalent width of the Li I line is so large that it lies on the saturated part of the curve of growth, where small errors in the equivalent width correspond to large errors in the inferred Li abundances. Therefore high Li abundances deduced from curve of growth analysis of the 6707.81 Å line may be affected by systematic errors. In fact some PMS objects have Li abundances deduced from the analysis of the 6707.81 Å line that are significantly in excess of $\log n(\text{Li})=3.0$, i.e. higher than the currently accepted primordial Li abundance. In the case of the T-Tauri star BP Tauri, Duncan (1991) has shown that the very high Li abundances deduced from the 6707.81 Å line which have appeared in the literature are not substantiated by a careful analysis of the weaker (and therefore not saturated) Li I 6103 Å line, the “true”

abundance being close to $n(\text{Li})=3.0$. Nevertheless, the bulk of the available data on Li abundances currently rests on values obtained by curve of growth analyses of the 6707.81 Å line, which, independently of the absolute accuracy of the method, do form a fairly homogeneous data sample that can be used for ‘relative’ analysis.

Although the lithium abundance is one of the “classical” stellar age indicators (Herbig 1965), the strict correlation of Li abundance with stellar age has in more recent years been questioned by several observations. Among the most prominent are the observation of a more or less constant Li abundance in Pop II stars (Spite 1990), the observation of isolated disk giants with Li abundances much higher than implied by their evolutionary age (Gratton & D’Antona 1989), the detection of the “hiatus” in Li abundances in the Hyades F stars (Boesgard 1987) and the recent observations of high Li abundances in evolved active star systems such as RS CVn binaries (Pallavicini et al. 1992). All these observations have contributed to show that the traditional picture of Li being uniformly depleted with time in stars with a high enough temperature at the base of the convection zone is too simplistic. Several mechanisms have been invoked to ex-

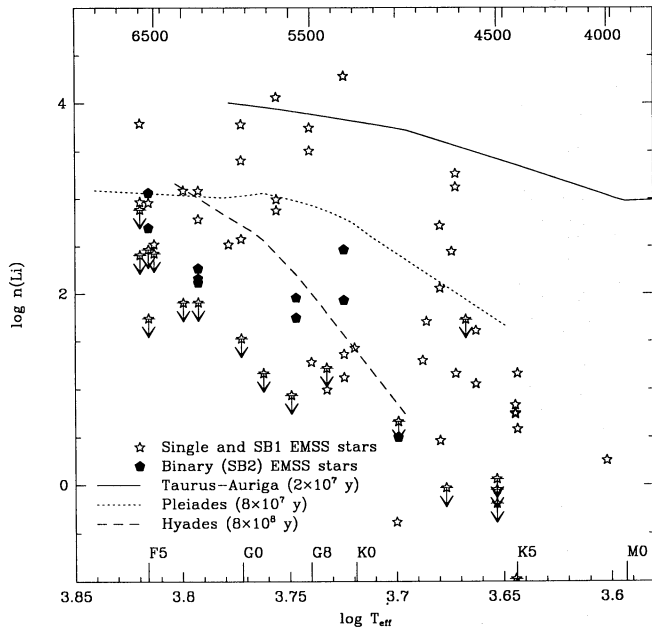


Fig. 3. Li abundances for the subsample of Extended Medium Sensitivity Survey described in the text computed using a curve of growth analysis, plotted against $\log(T_{\text{eff}})$, together with robust fits to the Li abundances for the Hyades, Pleiades and Tau-Aur samples. Single (or SB1) systems are identified by open symbols, binary (SB2) systems by filled symbols (each component is plotted separately at the same T_{eff}). Upper limits to the Li abundance are identified by down-pointing arrows

plain the observed anomalies. For example, in the case of the high Li abundances in active stars, a variety of mechanisms, including the production of Li during coronal flares through spallation reactions, and lower effective temperature of a star with a large spotted surface (as it can be expected on a very active star) have been invoked as possible explanations for the anomalous Li abundance (Pallavicini et al. 1992), although Pallavicini et al. (1993) have recently shown that star spots cannot be a viable explanation for anomalously strong Li lines sometimes observed in RS CVn binaries. Additionally, based on a re-analysis of the data of Pallavicini et al. (1993), Randich et al. (1993) have recently shown that objects with high Li abundances, in excess of 1.5 (that is, above the “Pleiades” line in Fig. 2), are most easily explained in terms of their actually being young.

We believe that our sample cannot be affected by a large number of giants, because on the basis of their X-ray luminosity function (Maggio et al. 1990), we predict with the X-ray Galaxy model of Favata et al. (1992) that only a small number of serendipitous giants must be detected in the EMSS. Furthermore we have rejected most of the known RS CVn from our sample, to minimize the contamination of this class of objects. The selection criteria of our sample are very different from the sample, for example, of Pallavicini et al. (1992) (which, as shown by Randich et al. (1993) is quite heterogeneous), where most of the stars are either active stars or giants. It is therefore likely that the two samples have a substantial difference in composi-

tion. For these reasons we believe that the majority of our high lithium stars are actually young stars.

In what follows we will compare the Li abundances for our sample stars with the Li abundances for known age-homogeneous samples of stars obtained through the same type of curve of growth analysis. It can be seen from Fig. 3 that the Li abundance distribution in our sample is nothing like the Li abundance distribution of randomly selected Pop I disk stars (which would, in Fig. 3 be distributed mostly below the Hyades line), as our sample contains a much larger fraction of high Li stars. This is not a posteriori an unexpected fact, given the known dependence of X-ray luminosity on stellar age and the recently observed high lithium abundances in evolved active stars. The comparison of X-ray luminosity functions of age-homogeneous groups of stars (Vaiana et al. 1992, Sciortino 1993) has clearly shown that, for coronal sources, the average X-ray luminosity within a given spectral type decreases with age. It is therefore likely that, in an X-ray flux limited sample such as the EMSS, the age distribution of the sample should be biased toward young ages with respect to the age distribution of the general Pop I disk population, which will contain a large fraction of older and therefore X-ray inactive stars (Micela et al. 1993).

6. Discussion

The observations presented here fully support the original hypothesis that prompted them, namely that a large fraction of the the program stars are rather young objects. In addition, a sizable fraction (10 objects out of 67, or about 15 %) have very high lithium abundances, consistent with their being pre-main sequence (PMS) objects. Given the lack of any other macroscopic spectral peculiarities in most of them, it seems likely that these belong to the same class of objects as the naked T-Tauri stars of Walter et al. (1988) (also called weak-line T-Tauri stars). The fraction of PMS candidates detected in the present work is much higher than what would be expected from a survey of randomly selected field stars. This shows that PMS are an important (and perhaps so far underestimated) contributor to the X-ray sky in the flux range $2.0 \cdot 10^{-12} - 7.1 \cdot 10^{-14} \text{ erg}/(\text{cm}^2 \text{ sec})$.

One of the constraints of the EMSS is that it only covers the high galactic latitude ($|b| > 20 \text{ deg}$) sky. It is therefore even more remarkable that it contains so many very young coronal sources, given that star formation regions are usually found close to the galactic plane. Furthermore, with two exceptions, which most likely belong to the Ophiucus star formation region, all the high lithium stars in our sample appear to lie outside of known star formation regions, and to be spread around in the sky. It does therefore appear that substantial numbers of isolated X-ray luminous PMS stars exist, with no apparent connection to known star formation regions. This result also confirms that detailed study of coronal X-ray sources is a very efficient technique for finding PMS candidates outside known star formation region.

We are planning an extension of the present work to the fainter magnitude end of the stellar component of the EMSS. This would provide both an estimate of the spatial density of PMS in our galactic neighborhood, and an estimate of their true

X-ray luminosity function. This in turn could be used to put strong constraint on the recent history of star formation rate in the Galaxy, using the method of Micela et al. 1993. Additionally, we are planning a detailed follow-up work on the most interesting of the sources detected here (specially the candidate PMS), which will include optical and IR ground based observations, and UV and X-ray observations. Finally, it will be interesting, when the Hipparcos astrometric results will be available, to study the space motion of the several PMS candidates detected, to see whether they appear to have formed in known star formation regions.

7. Summary and conclusions

We have presented lithium abundances determined by the method of the curve of growth from high resolution spectra of the Li 6708 Å line for a large sub-sample of the “yellow” stars in the Extended Medium Sensitivity Survey. The observations presented here were prompted by the need for a better understanding of the age distribution of coronal X-ray sources in the *Einstein* Extended Medium Sensitivity Survey. A relatively high fraction of the observed sources have Li abundances compatible with their being objects still in the pre-main sequence stage, which points to their being naked T-Tauri stars (Walter et al. 1988). A large part of the others stars has lithium abundance compatible with that of young stars, such as the Pleiades, just arrived on the main sequence. Although the limited apparent magnitude coverage of our sample with respect to the full Extended Medium Sensitivity Survey sample prevent a strict statistical analysis, the fraction of very young sources present in our sample is consistent with the hypothesis of Micela et al. (1993), that such an unbiased X-ray selected sample must contain a large fraction of very young sources. Therefore we conclude that very young sources (and more in general stars with a high Li abundance) are important contributors to X-ray source counts in the X-ray flux range $2.0 \cdot 10^{-12} - 7.1 \cdot 10^{-14} \text{ erg}/(\text{cm}^2 \text{ sec})$.

Acknowledgements. G.M. and S.S. acknowledge financial support from ASI (Italian Space Agency), and MURST (Ministero della Università e della Ricerca Scientifica e Tecnologica). The Simbad database was extensively used to prepare the observations presented here. The IRAF software system was used for the data reduction. We would like to thank the staff of ESO and DAO observatories for their dedicated support throughout the observation program. We thank P. Jakobsen, A. Maggio, R. Pallavicini, G. Peres, and S. Serio and our referee (T. Fleming) for their helpful comments. Last, we would like to thank T. Maccacaro for having supplied us finding charts for some of the EMSS sources in advance of publication.

Appendix A: notes on individual stars

Note: the spectra plotted here are all normalized to a relative intensity of the continuum of 1.0. The wavelength units are all Å. The wavelength scale is not corrected for the stellar radial velocity.

MS 0003.3-4201: this star, due to its southern latitude, is not included in the sample of Fleming (1988) (the same is true

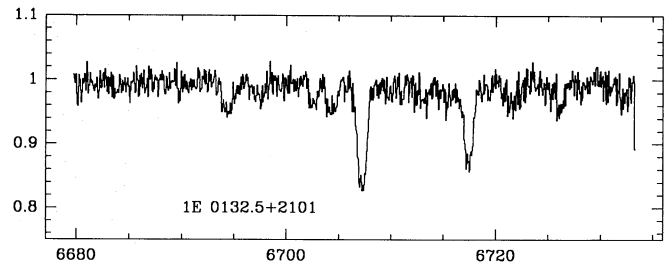


Fig. 4. Li region spectrum for MS0132.5+2102

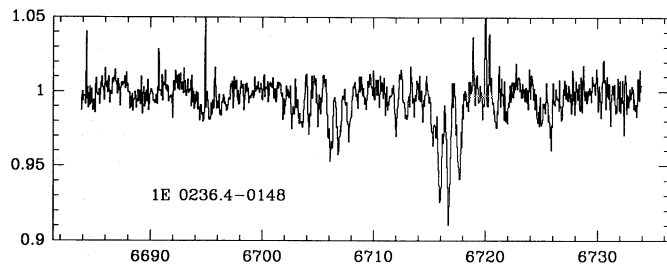


Fig. 5. Li region spectrum for MS 0236.4-0148

for many other stars in our sample). No peculiarities about it are known from the literature. Nevertheless its deep Li line implies a Li abundance well in excess of 3.0, which, for a G0 star, makes it a likely PMS candidate.

MS 0009.9+1417: this star was part of the original Medium Sensitivity Survey. It is a binary, with a period of few days, and it has been observed by IUE by Bergoffen et al. (1988). It shows strong emission in all of the prominent chromospheric lines, and it was classified by Fleming (1988) as a probable RS CVn object. Its Li abundance is not exceptional for an RS CVn type binary (Randich et al. 1993).

MS 0132.5+2101: classified as a normal star by Fleming (1988), this star is a relatively fast rotator, with a deep Li line, and an computed Li abundance above 3.5. According to Fleming (1988) this object does not show any evidence of multiplicity. A very strong PMS candidate. The spectrum is shown in Fig. 4.

MS 0134.4+2027 already classified as a binary system by Fleming (1988), it shows two clearly separated spectral systems. The Li line can be separately measured for the two components. The deduced Li abundances are within the expected uncertainty of each other, therefore supporting the assumption of similar stellar components. This object was also detected in the EXOSAT High Latitude Survey.

MS 0236.4-0148: this star was not in the original sample of Fleming (1988). Three clearly separated spectral systems are evident in the spectrum, and the Li equivalent width can be measured easily for each of the components. The deduced Li abundances for all the components are equal to within the expected uncertainty. The assumption of similar temperature and radius for each of the component seems therefore valid. The spectrum is shown in Fig. 5.

MS 0300.1-1528: although classified as single star by Fleming (1988) (on the basis of only two radial velocity measure-

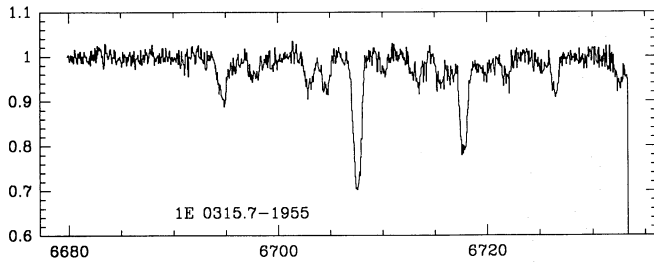


Fig. 6. Li region spectrum for MS 0315.7-1955

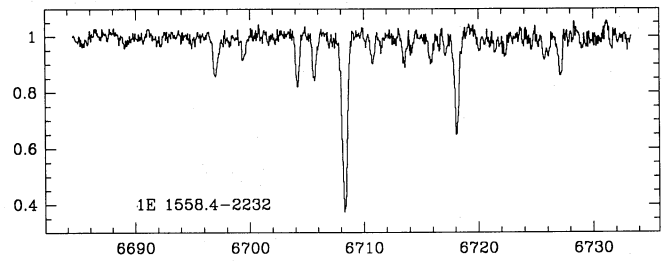


Fig. 7. Li region spectrum for MS 1558.4-2232

ments) our spectrum shows two clearly separated spectral systems, with identical (within the expected uncertainty) small Li equivalent widths, therefore supporting the assumption of similar stellar components.

MS 0307.5+1424: classified as a normal G6V single star by Fleming (1988), it has a very deep Li absorption line, with an implied Li abundance in excess of 3.5. A PMS candidate.

MS 0315.7-1955: an SB1 binary system, classified as an RS CVn candidate by Fleming (1988) on the basis of the multiplicity coupled with a relatively high rotational velocity ($v \sin(i) = 23$ km/s). It displays a deep Li absorption feature, implying a Li abundance well in excess of 3.5. Therefore we consider it more likely to be a PMS candidate. The spectrum is shown in Fig. 6.

MS 0348.2-1404: already classified as binary by Fleming (1988), the two spectral systems are distinguishable in our spectra and the Li equivalent widths can be individually determined. The abundances derived from the assumption of equal components are not within the assumed uncertainty. Therefore the two stars in the system are likely to be significantly different in temperature and radius.

MS 0438.5+0213: there is a discrepancy between the spectral type (F9V) and the color index (0.85) reported by Fleming (1988), in that the color index is too red for the quoted spectral type. The Li abundance has been computed on the basis of the color index. Fleming (1988) considers this a candidate RS CVn. The object shows no detectable Li absorption line.

MS 0448.4+1058: the spectral lines in our observation are apparently single, but McAlister et al. (1990) report a close companion (of unreported magnitude) at 0.1 arcsec detected by speckle observations. This companion has surely contributed to our observed spectrum, given our slit width much larger than 0.1 arcsec. It cannot be excluded that the companion is in phase and is contributing substantially to the spectrum. The Li abundance might be therefore affected by a substantial error.

MS 0515.4-0710: not in the sample of Fleming (1988), this system is assigned a spectral class of K2e by Stocke et al. (1991). The spectrum shows a deep Li absorption feature, with an implied Li abundance in excess of 2.5, which, together with the presence of emission features in the spectrum, makes it a likely young star.

MS 0519.3-4544: one of the reddest objects in the sample, it is classified as K8Ve by Stocke et al. (1991). The equivalent width of the Li line is relatively large for an object of such

low effective temperature, although, given that the quoted abundance is based on an extrapolation from the available curves of growth, the inferred Li abundance is perhaps to be treated with caution.

MS 0535.7-2839: this star is not in the sample of Fleming (1988). The spectrum shows a deep, rotationally broadened Li absorption feature, with an equivalent width of about 0.120 Å. Together with an assumed effective temperature of 6500 K, deduced from the spectral type, this implies a very high Li abundance, in excess of 3.5, although for such a hot system a more precise determination of the effective temperature would be appropriate. In any case a PMS candidate.

MS 0617.0-5847: again an object not included in the sample of Fleming (1988). The spectrum shows absorption lines with a shape which could be due to the superposition of two spectral systems, one with narrow lines and one with somewhat broader lines. A Li absorption feature is evident, with an equivalent width normal for a star of this spectral class (F5V). A suspected multiple system.

MS 0648.1-5042: not in the sample of Fleming (1988). The spectrum shows a strong Li absorption feature with a large rotational broadening. The implied Li abundance, in excess of 3.0, coupled with the low assumed effective temperature, makes this object a candidate PMS.

MS 1520.7-0625: classified as an RS CVn type system by Fleming (1988).

MS 1552.0-2338: not in the sample of Fleming (1988), this star shows a deep Li absorption feature and a large rotational velocity. Although classified as G3IV, it is most likely a very young object (perhaps a PMS) and not an evolved one.

MS 1558.4-2232: not in the sample of Fleming (1988), this system was assigned a spectral class of K3e by Stocke et al. (1991). The spectrum shows a deep Li absorption feature, with an implied Li abundance in excess of 3.0, which, together with the presence of emission feature in the spectrum, makes it a likely PMS candidate. The spectrum is shown in Fig. 7.

MS 1737.2+6847: this bright star is a known spectroscopic binary. Both spectra are clearly visible, and both Li lines are separately measurable. The Li abundances deduced on the assumption of similar components are marginally within the assumed uncertainty, and should therefore not be taken at face value. A more accurate determination of the effective temperatures of the two components would be appropriate.

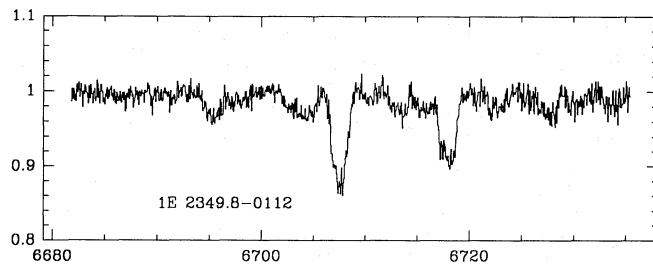


Fig. 8. Li region spectrum for MS 2349.8-0112

MS 1751.0+7045: a FK Com candidate of Fleming (1988). Its Li spectrum has been published by Ambruster et al. (1992), who report a revised spectral classification of K0III (revised from K5IV) and a Li equivalent width of 90 mÅ, which they translate to an abundance of 1.6, substantially in agreement with the observation presented here. In our spectrum the Li line is blended with the Fe line. On the basis of the estimated distance from the galactic plane ($178\text{pc} < z < 257\text{pc}$) Ambruster et al. (1992) considers this an evolved object. They also report IUE observations of this object which show high (close to saturation) chromospheric fluxes. While still relatively high for an evolved object, this Li abundance is by no means exceptional. It seems likely that this object is of a different sort than the other FK Com candidate present in our sample (MS2349.8-0112), which shows a much higher Li abundance.

MS 2349.8-0112: Fleming (1988) considered this object to be a candidate FK Com type object. He assigned it a spectral type of K0III (corresponding to $T_{\text{eff}} = 4500\text{ K}$), with the luminosity class assigned on the basis of the detection of the SrII 4077 Å line detected in a single low resolution spectrogram. On the other hand he gives a B-V color for this object of 0.70, corresponding to a much hotter type star ($T_{\text{eff}} = 5600\text{ K}$). This star has a very strong Li line (equivalent width greater than 0.2 Å), which would correspond to a Li abundance typical of a PMS object for either effective temperature. Therefore we consider this object to be a likely PMS candidate, rather than an FK Com. In table 5 this object is included twice, showing the Li abundance computed with both assumed values of T_{eff} . The spectrum is shown in Fig. 8.

References

- Ambruster, C., Fekel, F. and Guinan, E., 1992 in "Cool Stars, Stellar Systems and the Sun", Giampapa M. and Bookbinder J. eds, p. 569
 Basri, G., Martin, E., Bertout, C., 1991, A&A 252, 625
 Bergoffen, M., Stocke, J., Walter, F., Fleming, T., 1988, PASP 100, 736
 Boesgaard, A., 1987, ApJ 321, 967
 Cleveland, B., 1979, J. American Stat. Assoc. 74, 829
 Duncan, D., Jones, B., 1983, ApJ 271, 663
 Duncan, D., 1991, ApJ 373, 250
 Favata, F., Micela, G., Sciortino, S., Vaiana, G.S., 1992, A&A 256, 86
 Fleming, T., 1988, Ph.D. Thesis, Univ. of Arizona
 Fleming, T., Gioia, I., Maccacaro, T., 1989a, AJ 98, 2, 692
 Fleming, T., Gioia, I., Maccacaro, T., 1989b, ApJ 340, 1011
 Gratton, R., D'Antona, F., 1989, A&A 215, 66
 Herbig, G., 1965, ApJ 141, 588

- Maggio, A. et al., 1990, ApJ 348, 253
 McAlister, H., Hartkopf, W., Franz, O., 1990, AJ 99, 965
 Micela, G., Sciortino, S., Favata, F., 1993, ApJ in press
 Pallavicini, R., Cerruti-Sola, M., Duncan, D.K., 1987, A&A 174, 116
 Pallavicini, R., Cutispoto, G., Randich, S., Gratton, R., 1993, A&A 267, 145
 Pallavicini, R., Randich, S., Giampapa, M., 1992, A&A 253, 185
 Randich, S., Gratton, R., Pallavicini, R., 1993, A&A submitted
 Sciortino, S., 1993, in "Physics of Solar and Stellar Coronae", J. Linsky and S. Serio, eds., Kluwers Acad. Pub., in press
 Stocke, J., Morris, S., Gioia, I. et al., 1991, ApJS 76, 813
 Spite, F., 1990, Mem. S.A.It. 3, 663
 Vaiana, G.S., Maggio, A., Micela, G., Sciortino, S., 1992, Mem.S.A.It. 63, 3/4, 545
 Walter, F.M., Brown, A., Mathieu, R.D., Myers, P.C., 1988, AJ 96, 1, 297
 Zombeck, M., in *Handbook of Space Astronomy & Astrophysics, 2nd ed.*, Cambridge Univ. Press, Cambridge 1990, p. 68